2.L

Nuclear Physics **A108** (1968) 316—324;

DIFFERENTIAL CROSS SECTION AND POLARIZATION IN p-α SCATTERING FROM 22 TO 25 MeV

P. DARRIULAT †, D. GARRETA, A. TARRATS and J. TESTONI ††

Centre d'Etudes Nucléaires de Saclay

Received 5 October 1967

Abstract: The proton differential cross section and polarization in p-α scattering have been measured at 12 lab scattering angles from 20° to 155° for proton energies between 22 and 25 MeV. The resonance corresponding to a $\frac{3}{2}^+$ state of ^{5}Li is clearly observed. An energy-dependent phase-shift analysis of most of the available p-α scattering data between 20 and 27.8 MeV was made.

The energy dependence of the phase shifts was expressed in term of the resonance parameters with the Breit-Wigner single-level formula for the resonant part, and it was assumed to be linear for the non-resonant part. The resonance is well reproduced for both cross section and polarization.

E NUCLEAR REACTIONS ^{4}He(p, p), E = 22-24.8 MeV; measured $\sigma(E;\theta)$, polarization $(E;\theta)$. Deduced scattering phase shifts, ^{5}Li resonance parameters. Natural target.

1. Introduction

Recently, p-α experiments [1,2]) at proton energies between 20 MeV and 30 MeV have been performed in order to determine to what extent the p-α interaction is affected by the ^{4}He(p, d)^{3}He reaction threshold at 23.02 MeV (16.39 MeV in ^{5}Li) and the $\frac{3}{2}^+$ excited state in ^{5}Li at 16.64 MeV excitation energy.

Phase shifts have been obtained from cross section and polarization data and resonance parameters, deduced from reaction experiments, have been tested in the corresponding analysis [1]).

The aim of the present work is to increase the number of available cross-section and polarization data in order to have a better description of both angular distributions and excitation functions in the relevant energy region. Measurements for 12 angles from 20° to 155° at energies spaced by about 200 keV between 22 MeV and 25 MeV are reported. A phase-shift analysis including most of the available data is presented, and the accuracy of phase shift and resonance parameters is discussed.

2. Experimental arrangement

The proton beam of the Saclay variable energy cyclotron was used. The characteristics of the polarized beam are described in refs. [3,4]). Its polarization and intensity

† Now at CERN, Geneva, Switzerland.

†† IAEA Fellow on leave from CNEA, Laboratorio del Sincrociclotron Buenos-Aires, Argentina.

were of the order of 50 to 70 % and 1 to 2.10^8 protons/sec, respectively. The energy of the protons of the unpolarized beam (used for cross-section measurements) was determined by measuring their range in aluminium [5]). Multiple-scattering corrections were taken into account and, assuming that there is no uncertainty in the values given by the range-energy tables, the energy was known to about 50 keV. These measurements were used to calibrate the beam energy to cyclotron frequency relationship which was in turn used to obtain the energy of the polarized beam. This determination was in good agreement with a direct measurement obtained from the kinematics, the latter giving unfortunately a poor accuracy.

The gas target was filled with helium at room temperature under a pressure of 4 atm, the entrance and exit walls were 6.1 mg and 12.6 mg havar foils, respectively.

Six independent lithium-drifted silicon counters were used to detect protons scattered from the target. The angles of detection were set with an accuracy better than 0.05°. Slits for these detectors defined rms angular acceptances of $\Delta\theta = 1.8°$ for polarization measurements and for cross-section measurements of $\Delta\theta = 0.25°$ at scattering angles up to 52° and $\Delta\theta = 0.5°$ at larger angles.

The rms total energy spread (target thickness and beam energy) for polarization measurements varied from $\Delta E = 38$ keV at $\theta = 89°$ to $\Delta E = 55$ keV at $\theta = 20°$. In cross-section measurements, the target thickness was negligible and $\Delta E = 35$ keV.

For polarization measurements, after passing through the gas target, the beam was refocussed by a pair of quadrupole magnets on a carbon polarimeter of the same geometry as the one calibrated by Craig *et al.* [6]) at 15.6 MeV (centre of the target). The polarimeter was calibrated versus energy using this point for absolute normalisation. Before entering the polarimeter, the beam passed through an aluminium foil to be in an energy region where the polarization is high (14 to 17 MeV).

Asymmetries were obtained by flipping the beam polarization as described in ref. [4]).

3. Results

Values obtained for differential cross sections and polarizations are given in table 1 and fig. 1, respectively. They are uncorrected for the energy spread. Correction for finite angular acceptance was calculated as described in ref. [7]) but was found to be negligible for both polarization and cross section. The quoted uncertainties include statistical and systematic errors (for polarization they include, in particular, the error in the calibration of the polarimeter); in the cross section, they are relative and are given in percent. The energies E_p are the beam energies at the centre of the target.

4. Energy-dependent phase-shift analysis

We report a phase-shift analysis of the following sets of data:

(a) four differential cross-section angular distributions [2]) at 20.62, 23.34, 26.08 and 27.68 MeV proton energies (202 points),

TABLE

Differential cross section (in mb/sr) and polarization

E_p (MeV)	ψ lab = 20.0 $\theta_{c.m.}$ = 25.0	31.7 39.4	44.6 55.0	52.1 64.0	64.0 77.3	76.0 90.3
22.15	168.8±3.3	132.8±3.4	89.9±3.3	66.1±3.2	37.1±3.5	18.0 ±3.6
22.41	163.8±3.3	133.4±3.3	87.8±3.2	63.8±3.2	35.7±3.5	17.1 ±3.9
22.74	165.3±3.6	133.0±3.3	86.6±3.3	64.1±3.3	34.2±4.1	17.0 ±3.6
22.93	165.8±3.3	133.3±3.3	91.0±3.4	61.9±3.3	35.8±3.5	16.6 ±3.7
23.06	170.8±3.3	135.2±3.3	86.6±3.1	61.7±3.2	34.0±3.3	16.2 ±3.5
23.15	182.2±3.3	138.2±3.2	84.1±3.3	59.1±3.2	31.0±3.3	14.47±3.7
23.25	201.6±3.2	144.7±3.2	84.3±3.2	61.1±3.2	28.1±3.3	13.21±4.4
23.38	189.8±3.1	140.3±3.3	82.1±3.2	56.7±3.1	27.5±3.2	12.90±3.3
23.59	172.0±3.2	132.7±3.2	80.2±3.2	55.7±3.1	28.3±3.2	13.27±3.3
23.85	170.4±3.1	130.1±3.1	80.9±3.1	56.5±3.1	29.3±3.1	13.87±3.2
24.04	168.4±3.6	126.7±3.4	78.1±3.2	56.8±3.3	28.2±3.5	13.48±3.8
24.25	162.4±3.3	125.9±3.3	77.2±3.4	55.5±3.2	28.5±3.4	13.47±3.7
24.78	159.3±3.4	121.1±3.4	74.2±3.4	53.2±3.4	27.5±3.3	13.31±4.0
22.15	−0.116±0.007	−0.222±0.009	−0.338±0.009	−0.394±0.014	−0.502±0.021	−0.504±0.037
22.41	−0.141±0.009	−0.200±0.013	−0.331±0.011	−0.400±0.015	−0.558±0.039	−0.503±0.061
22.66	−0.140±0.006	−0.234±0.008	−0.349±0.013	−0.418±0.017	−0.479±0.024	−0.593±0.038
22.93	−0.163±0.007	−0.268±0.009	−0.399±0.011	−0.583±0.013	−0.558±0.026	−0.528±0.042
23.06	−0.160±0.021	−0.284±0.027	−0.464±0.035	−0.475±0.046	−0.673±0.089	−0.431±0.142
23.19	−0.098±0.008	−0.169±0.010	−0.309±0.013	−0.413±0.019	−0.517±0.032	−0.529±0.055
23.32	−0.034±0.012	−0.116±0.019	−0.223±0.030	−0.390±0.040	−0.605±0.065	−0.677±0.104
23.46	−0.052±0.002	−0.111±0.009	−0.213±0.015	−0.295±0.021	−0.442±0.030	−0.654±0.049
23.59	−0.070±0.019	−0.122±0.029	−0.120±0.040	−0.328±0.050	−0.373±0.090	−0.503±0.148
23.72	−0.051±0.009	−0.102±0.013	−0.198±0.012	−0.286±0.016	−0.520±0.043	−0.575±0.064
23.85	−0.043±0.019	−0.106±0.026	−0.244±0.036	−0.293±0.046	−0.449±0.084	−0.685±0.135
23.99	−0.035±0.009	−0.067±0.014	−0.202±0.017	−0.306±0.023	−0.468±0.041	−0.647±0.066
24.25	−0.069±0.009	−0.120±0.011	−0.205±0.011	−0.269±0.016	−0.441±0.039	−0.553±0.059
24.78	−0.067±0.012	−0.114±0.014	−0.175±0.025	−0.233±0.032	−0.384±0.048	−0.617±0.075

The cross section errors are relative and given in percent.

(b) two differential cross-section excitation curves [2]) between 20 and 27.8 MeV (89 points),

(c) six polarization excitation curves [1]) between 20 and 27 MeV (64 points),

(d) 12 differential cross-section excitation curves (this work) between 22 and 25 MeV (156 points) and

(e) 12 polarization excitation curves (this work) between 22 and 25 MeV (168 points).

4.1. PARAMETRIZATION OF THE PHASE SHIFTS

Differential cross sections and polarizations are expressed as a function of the scattering amplitudes in the usual way, the amplitudes being expanded in partial waves up to F-waves inclusively.

We attempt to reproduce the experimental data with phase shifts depending linearly upon the energy except for the $D_{\frac{3}{2}}$ phase shift to which we add a resonant part

1
versus incident proton energy for 12 scattering angles

89.0 104.1	102.4 116.9	111.9 125.5	129.7 141.0	142.0 151.0	155.0 161.2
7.05±3.8	5.18±3.1	7.09±4.0	16.1 ±3.5	22.4±4.1	28.6±3.9
6.99±3.7	4.47±3.8	7.12±4.0	15.22±4.0	21.3±3.9	27.0±3.9
6.74±4.5	4.41±5.2	6.61±7.4	14.01±8.1	20.3±6.8	25.3±5.4
6.95±3.9	4.71±3.8	6.91±4.3	14.65±3.4	20.0±3.9	24.7±4.0
6.65±3.7	4.70±3.7	6.71±3.9	14.04±4.1	19.0±3.8	23.6±4.0
6.93±3.7	5.96±3.5	8.05±3.9	13.31±3.8	16.3±3.6	19.1±4.3
7.29±3.5	7.60±3.7	9.60±3.6	13.58±3.4	15.8±5.3	18.1±7.2
7.44±3.4	8.43±3.3	10.61±3.3	14.48±3.2	16.0±4.3	17.2±3.5
6.97±3.4	7.66±3.3	9.70±3.4	14.72±3.2	17.5±3.5	20.2±3.8
6.55±3.3	7.21±3.3	9.25±3.2	14.78±3.2	18.2±3.3	21.2±3.4
6.90±4.2	6.50±4.0	8.65±5.3	13.74±4.4	16.7±8.1	20.2±4.0
7.59±3.6	6.58±3.9	8.47±4.1	13.62±3.6	16.8±6.0	19.6±9.1
6.62±3.7	6.38±3.8	8.04±4.0	13.42±3.6	16.0±4.9	20.2±9.7
−0.310±0.058	+0.747±0.070	+0.940±0.058	+0.553±0.044	+0.347±0.032	+0.185±0.025
−0.291±0.060	+0.714±0.071	+0.979±0.010	+0.489±0.077	+0.291±0.034	+0.148±0.024
−0.220±0.068	+0.748±0.077	+0.825±0.063	+0.445±0.049	+0.296±0.038	+0.122±0.030
−0.104±0.064	+0.707±0.079	+0.679±0.075	+0.266±0.052	+0.100±0.037	+0.081±0.028
−0.257±0.174	+0.876±0.191	+0.377±0.234	+0.420±0.172	+0.068±0.117	−0.037±0.090
−0.196±0.071	+0.690±0.071	+0.739±0.057	+0.366±0.057	+0.264±0.048	+0.159±0.040
−0.449±0.144	+0.637±0.144	+0.942±0.128	+0.795±0.104	+0.392±0.097	+0.384±0.079
−0.119±0.074	+0.459±0.076	+0.673±0.066	+0.682±0.053	+0.518±0.047	+0.309±0.038
−0.452±0.175	+0.277±0.187	+0.859±0.184	+0.794±0.145	+0.476±0.111	+0.437±0.092
−0.226±0.079	+0.612±0.079	+0.918±0.087	+0.639±0.070	+0.551±0.045	+0.349±0.038
−0.479±0.158	+0.777±0.179	+0.954±0.168	+0.900±0.146	+0.484±0.109	+0.338±0.084
−0.234±0.080	+0.645±0.087	+0.942±0.086	+0.767±0.070	+0.567±0.049	+0.253±0.041
−0.284±0.058	+0.565±0.065	+0.751±0.065	+0.710±0.065	+0.612±0.037	+0.338±0.028
−0.278±0.122	+0.729±0.128	+0.728±0.111	+0.692±0.084	+0.636±0.074	+0.446±0.059

expressed by the Breit-Wigner single-level formula in terms of four resonance parameters. Denoting $\delta_l^{\pm}$ the complex phase shift of orbital angular momentum l and total angular momentum $j = l \pm \frac{1}{2}$, we have explicitly

$$\exp(2i\delta_l^{\pm}) = \tau_l^{\pm} \exp(2i\mu_l^{\pm})(1+R_l^{\pm}),$$

$$\tau_l^{\pm} = 1 \text{ below threshold } E \leqq E_{\text{th}} = 23.02 \text{ MeV},$$

$$\tau_l^{\pm} = 1 - \frac{\mathrm{d}\tau_l^{\pm}}{\mathrm{d}E}(E - E_{\text{th}}) \qquad E > E_{\text{th}},$$

$$\mu_l^{\pm} = \bar{\mu}_l^{\pm} + \frac{\mathrm{d}\mu_l^{\pm}}{\mathrm{d}E}(E - E_{\text{th}}),$$

where $\mathrm{d}\tau_l^{\pm}/\mathrm{d}E$, $\bar{\mu}_l^{\pm}$ and $\mathrm{d}\mu_l^{\pm}/\mathrm{d}E$ are parameters independent of energy; $R_l^{\pm}$ is zero

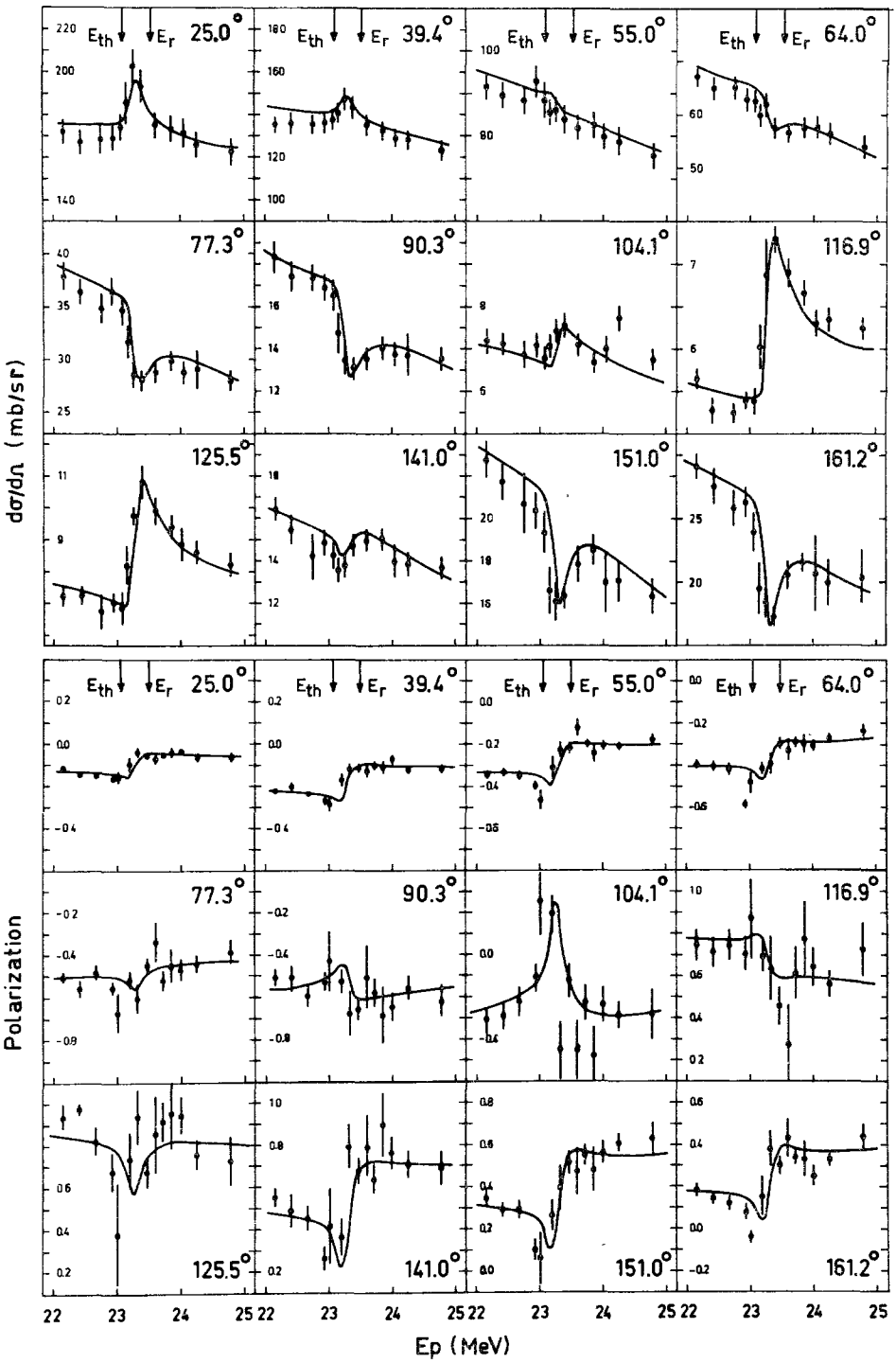

Fig. 1. The differential cross section (in mb/sr) multiplied by the scale factor $N_d = 1.02$ and the polarization are plotted versus the proton incident energy E_p for 12 centre-of-mass scattering angles. The curves are the phase shifts fit to the data calculated with the parameters of table 2.

except for $R_2^- = (\Gamma_p/(\Gamma_p+\Gamma_d))\ [\exp(2i\beta)-1]$, where

$$\beta = \mathrm{tg}^{-1}\frac{\Gamma_p+\Gamma_d}{2(\varepsilon_r+\Delta_p+\Delta_d-\varepsilon)},$$

$$\Gamma_i = 2\rho_i\gamma_i^2, \quad \Delta_i = -(S_i-B_i^c)\gamma_i^2, \quad i = p, d,$$

P_p, S_p, P_d and S_d are the penetration factors and level shifts in the proton and deuteron channels, respectively, calculated at radius r_0, E and ε the lab and centre-of-mass energies, respectively, B_p^c and B_d^c correspond to boundary conditions such that $\Delta_p+\Delta_d$ vanishes [8,9]) at the resonance energy E_r; $B_{p(d)}^c = S_{p(d)}(E_r)$ and γ_p^2 and γ_d^2 the reduced widths in the proton and deuteron channels, respectively.

4.2. LIMITATIONS ON THE PARAMETERS

Since between 23.02 MeV and 25.8 MeV, the only open inelastic channel is d + ^{3}He and assuming that below 27 MeV it remains the predominant one, it is possible to indicate limitations on some of the absorption parameters $d\tau_l^{\pm}/dE$.

The deuteron wave number k_d is small in the d + ^{3}He channel ($k_d = 0.41$ fm^{-1} at $E = 27$ MeV) so that the relative angular momentum l_d in this channel should only have the values 0 or 1. Therefore the system can only be in a parity and angular momentum state $\frac{1}{2}^+$, $\frac{3}{2}^+$, $\frac{1}{2}^-$, $\frac{3}{2}^-$ or $\frac{5}{2}^-$. Owing to parity and total angular momentum conservation, $d_{\frac{5}{2}}$ and $f_{\frac{7}{2}}$ waves cannot contribute to the inelastic channel, and the corresponding absorption parameters are therefore equal to zero throughout the analysis.

The quality of the fits is found very unsensitive to the channel radius r_0 as expected.

Two analyses are therefore undertaken, one with $r_0 = 5$ fm for comparison with previous works [1]) and the other with $r_0 = 10$ fm, which gives slightly better results †.

In all cases, γ_d^2 is very large and is even slightly superior to the Wigner limit $\gamma_W^2 = 3\hbar^2/2\mu r_0^2 = 3.15$ MeV. In order to satisfy the relation [9]) $\gamma_p^2+\gamma_d^2 \leqq \gamma_W^2$ and since the quality of the fits is found to be very little dependent on the absolute values of the reduced widths, γ_d^2 is kept equal to 3 MeV throughout the analysis. This large value of the d + ^{3}He reduced width seems reasonable for a resonance just above the corresponding threshold.

4.3. RESULTS

Using a standard χ^2 minimization method, the parameters are varied to give the best fit to the data of the sets (a)-(e) together.

Three further parameters N_a, N_b and N_d are introduced as scale factors common to all data of sets (a), (b) and (d), respectively. The best fit is obtained for

$$N_a = N_b = 1.00, \qquad N_d = 1.02.$$

† A reason why such a large d + ^{3}He channel radius may be reasonable is explained in ref. [10]), p. 367.

For sets (c) and (d), the experimental errors given in table 1 are combined with an error corresponding to a 50 keV uncertainty in the energy, but it was not attempted to correct for the energy spread.

The starting values of the parameters are from the analysis of Weitkamp and Haeberli [1]). Searches starting with values differing from those by a few "error bars" (as defined further) always converge to the same minimum, but no attempt was made to find a drastically different solution.

The set of parameters giving the best fit with $r_0 = 5$ fm is given in table 2. The corresponding excitation curves are shown on figs. 1 and 2. The agreement with the data is reasonably good, and the shape of the resonance is well reproduced at all angles for cross sections as well as for polarizations. The quality of the fit is the same for the different sets of data, and there is no appearance of systematic discrepancies between them.

TABLE 2

Parameters as defined in subsect. 4.1 giving the best fit to the data

	$d\tau/dE$ $(MeV)^{-1}$	$\bar{\mu}$ (deg)	$d\mu/dE$ $(deg \cdot MeV^{-1})$
$S_{\frac{1}{2}}$	$0.007 \pm 0.010(0.004)$	$86.9 \pm 1.0(0.4)$	$-1.1 \pm 0.5(0.2)$
$P_{\frac{1}{2}}$	$0.016 \pm 0.010(0.003)$	$52.0 \pm 0.5(0.2)$	$-0.1 \pm 0.2(0.1)$
$P_{\frac{3}{2}}$	$0.048 \pm 0.005(0.002)$	$89.6 \pm 0.6(0.2)$	$-0.1 \pm 0.3(0.1)$
$D_{\frac{3}{2}}$	$0.038 \pm 0.008(0.002)$	$5.5 \pm 0.4(0.2)$	$1.1 \pm 0.2(0.1)$
$D_{\frac{5}{2}}$	0.0	$9.0 \pm 0.4(0.2)$	$1.7 \pm 0.2(0.1)$
$F_{\frac{5}{2}}$	$0.001 \pm 0.005(0.002)$	$1.9 \pm 0.3(0.2)$	$0.6 \pm 0.2(0.1)$
$F_{\frac{7}{2}}$	0.0	$2.1 \pm 0.4(0.2)$	$0.4 \pm 0.2(0.1)$

γ_p^2 (MeV) $= 0.045 \pm 0.004(0.001)$, γ_d^2 (MeV) $= 3.0$,
$g = \gamma_d^2/\gamma_p^2 = 67 \pm 6(2)$, $r_0 = 5$ fm,
ε_R (MeV) $= 18.70 \pm 0.040(0.035)$.

The corresponding excitation curves are shown on figs. 1 and 2. The error bars are defined in subsect. 4.3.

Although the estimated reaction cross sections σ_{ex}^R given in ref. [1]) are not part of the data to be fitted, they are in excellent agreement with the reaction cross sections σ_c^R calculated from the phase shifts

at 26.08 MeV $\quad \sigma_c^R = 49$ mb, $\quad \sigma_{ex}^R = 47 \pm 4$ mb,

at 27.68 MeV $\quad \sigma_c^R = 64$ mb, $\quad \sigma_{ex}^R = 66 \pm 6$ mb.

The curve followed by the amplitude $f_2^- = (1/2i)\,(\exp[2i\delta_2^-] - 1)$ in the complex plane in the energy range of this analysis, is shown on fig. 3, the numbers refer to the proton bombarding energy in MeV.

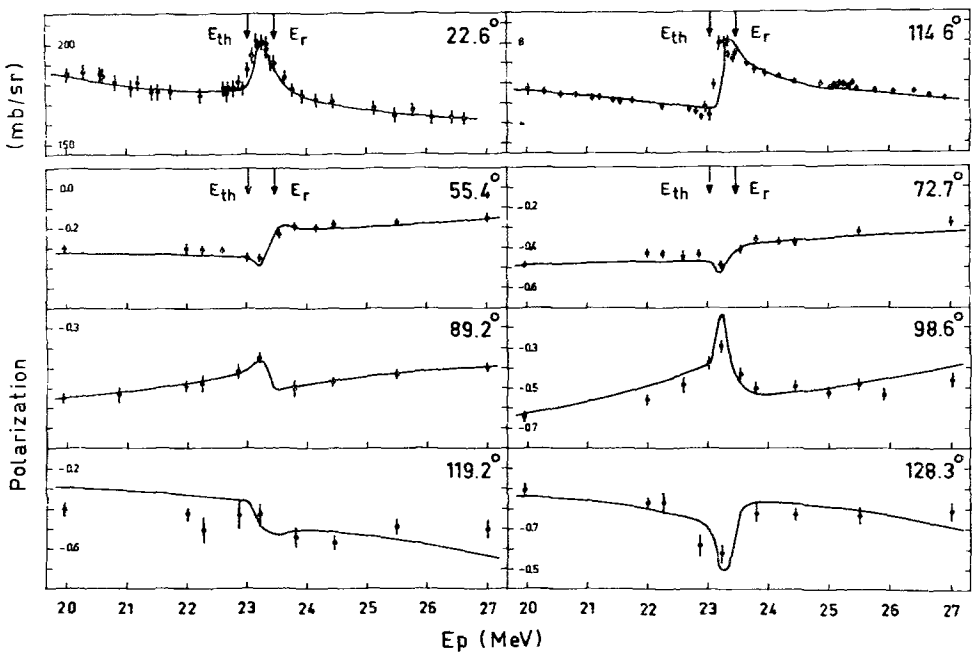

Fig. 2. The differential cross section (in mb/sr) of ref. [2]) and the polarization of ref. [1]) are plotted versus the proton incident energy E_p for two and six centre-of-mass scattering angles, respectively. The curves are the phase shifts fit to the data calculated with the parameters of table 2.

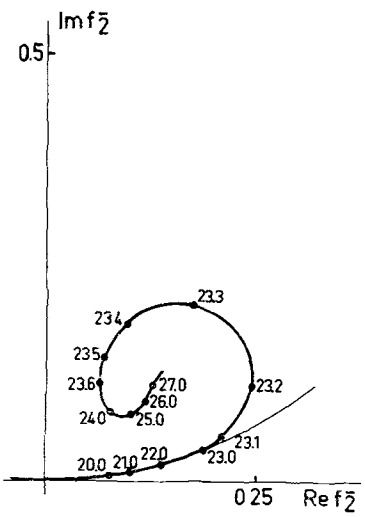

Fig. 3. The curve calculated with the parameters of table 2 is the actual path which f_2^- follows. The large circle is the unitary circle. The numbers refer to the proton bombarding energy in MeV.

The minimum χ^2 value obtained is 1600, although the expected value is 680. This corresponds to a rms deviation from the data of 1.54 standard deviation. A large contribution to the χ^2 comes from the points around 23.2 MeV (533 for 118 points) where there is a shift in energy of about 100 keV between the curves and the data; it is clearly visible on sets (b), (d) and (e). We could not find a set of resonance parameters, which made that shift disappear.

The "error bars" quoted on table 2 are figures that give an idea of the relative level of uncertainty in the determination of the different parameters. They correspond to the change in the parameter necessary to increase the minimum χ^2 value by 10 (leaving all the other parameters free). This value of the increase of the minimum χ^2, which has no basic justification, was chosen because all the searches that arrived to a reasonable fit gave a set of parameters inside the corresponding error bars. The figures in parentheses correspond to the change necessary to increase the χ^2 value by the same amount, when keeping all the other parameters fixed. The comparison with the corresponding error bars gives the amount of correlation in the determination of the parameter between the parameter and the rest of the set.

The differences between the phase shifts obtained in ref. [1]) at energies 20.62, 26.08 and 27.68 MeV and those calculated at these energies from the parameters of table 2 are of the order of one error bar. The resonance parameters of table 2 are almost identical to the first set of ref. [1]).

We would like to thank Dr. W. G. Weitkamp and Professor W. Haeberli for sending us their results of phase-shift analysis before publication and Dr. P. W. Allison and Professor R. Smythe for permitting us to see their p-α differential cross-section data in advance of publication.

References

1) W. G. Weitkamp and W. Haeberli, Nuclear Physics **83** (1966) 46
2) P. W. Allison and R. Smythe, private communication
3) P. Catillon, M. Chapellier and D. Garreta, Nuclear Physics **B2** (1967) 93
4) P. Kossanyi-Demay, R. de Swiniarski and C. Glashausser, Nuclear Physics **A94** (1967) 513
5) C. F. Williamson, J. P. Boujot and J. Picard, rapport CEA R-3042
6) R. M. Craig *et al.*, Nucl. Instr. **30** (1964) 268
7) E. A. Silverstein, Nucl. Instr. **4** (1959) 53
8) A. M. Lane and R. G. Thomas, Revs. Mod. Phys. **30** (1958) 323
9) T. Teichmann and E. P. Wigner, Phys. Rev. **87** (1952) 123
10) A. I. Baz, Advan. Phys. **8** (1959) 360